Supporting Information

Linker-Curvature Stabilized Zn–Rod Framework with Inverted C2 Hydrocarbon Adsorption

Xuan Han,[a] Wei Wang, [a] Jinli Zhu[a],Jin Wang*[a] and Mingxing Zhang*[a]*

[a] Nantong University, Nantong 226019, P. R. China

*(J.Z.). Email: jinlizhu@ntu.edu.cn.

*(J.W.). Email: wangjin110@ntu.edu.cn

*(M.Z.). Email: zmx0102@hotmail.com.

The Supporting Information provides experimental details and additional analyses supporting the mechanistic interpretation of inverted adsorption energetics discussed in the main text.

Experimental Details

Materials and Methods.

Commercially available reagents were directly used without further refinement. Powder X-ray diffraction (PXRD) data were tested on a Bruker axs D8 Advance diffractometer using Cu Kα radiation (λ = 1.5418 Å) over the 2θ range 5 ~ 45° with a routine power of 1600 W (40 kV, 40 mA) in a scan speed of 0.1 deg/s at room temperature.

Synthesis of Compound.

A mixture of $Zn(NO_3)_2 \cdot 4H_2O$ (30.0 mg, 0.10 mmol), pyrrole-2,5-dicarboxylic acid (15.0 mg, 0.05 mmol), melamine (8.0 mg, 0.041 mmol), and DMF (2 mL) was sealed in a 23 mL Teflon-lined stainless-steel autoclave and heated at 100 °C for 48 h. Red block crystals of **NTUniv-69A** were obtained, collected by filtration, and washed with DMF. Yield: 8.3 mg (76% based on pyrrole-2,5-dicarboxylic acid). Anal. Calcd for $[Zn(prdc)] \cdot (DMF) \cdot (H_2O)$: C 34.9%, H 3.9% and N 9.0%. Found: C 35.1%, H 4.0% and N 8.9%.

Melamine was introduced as a structure-directing and pH-modulating agent during the synthesis, helping to regulate the coordination environment and crystallization process. It is not incorporated into the final framework. Bulk samples were obtained by scaling up the synthesis through proportional increase of all reactants under identical conditions. The synthesis is reproducible and can also be performed in parallel batches, and the resulting products were combined for further use.

X-ray Crystallography.

Single-crystal X-ray diffraction data were measured on a Bruker Apex II CCD diffractometer using graphite monochromated Mo/Kα radiation (λ = 0.71073 Å). Data reduction was made with the Bruker SAINT program. The structures were solved by direct methods and refined with full-matrix least squares technique using the SHELXTL package. Non-hydrogen atoms were refined with anisotropic displacement parameters during the final cycles. Organic hydrogen atoms were placed in calculated positions with isotropic displacement parameters set to 1.2 × U_{eq} of the attached atom. The unit cell includes a large region of disordered solvent molecules, which could not be modelled as discrete atomic sites. We employed PLATON/SQUEEZE to calculate the diffraction contribution of the solvent molecules and, thereby, to produce a set of solvent-free diffraction intensities; structures were then refined again using the data generated. Crystal data are summarized in Table S1.

CCDC 2452318 contains the supplementary crystallographic data for **NTUniv-69A**. The data can be obtained free of charge at www.ccdc.cam.ac.uk/conts/retrieving.html or from the Cambridge Crystallographic Data Centre, 12, Union Road, Cambridge CB2 1EZ, UK.

Gas Adsorption Testing.

N_2, CO_2, C_2H_2, C_2H_4 and C_2H_6 sorption isotherms (up to 1 bar) were tested on Micromeritics ASAP 2060 surface area and pore size analyzer. In the preparation of gas sorption measurements, the **NTUniv-69A** was solvent-exchanged with acetone. After that, about 100 mg samples were pumped by using the "outgas" function of the surface area analyzer with turbo molecular pump. For all isotherms, warm and cold free space correction measurements were tested using ultra-high purity He gas of UHP grade 5.0 (99.999% purity). A part of the N_2 sorption isotherm at 77 K in the P/P_0 range 0.001–0.03 was fitted to the BET equation to figure out the BET surface area and the Langmuir surface area calculation was performed using all data points.

The pore size distribution (PSD) was obtained from the BJH model in the Micromeritics ASAP 2060 software package based on the N_2 sorption isotherm.

Breakthrough experiment.

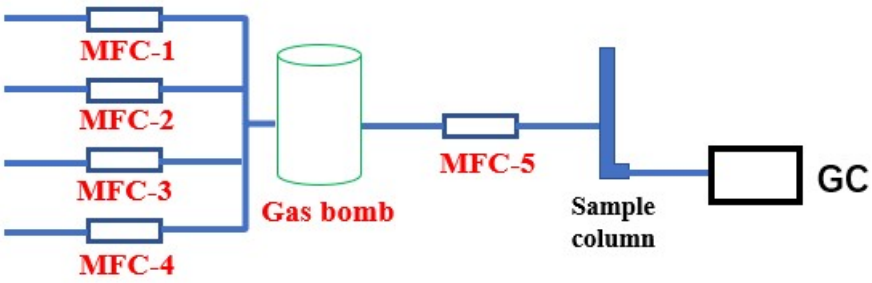

Figure S1. Schematic diagram of the custom-built testing apparatus for breakthrough experiments (MFC was Mass Flow Controller).

The breakthrough experiments were performed on a gas-separation apparatus which was designed and assembled by ourselves. In the breakthrough system. All flow rates of all gases can be regulated by the mass flow controllers. The breakthrough curves in this investigation were collected at 298 K. An activated sample of **NTUniv-69A** (1.243 g) in a stainless-steel column (0.40 cm internal diameter × 15 cm length) was used for testing and the remaining volume in the column was filled by glass wool. Helium gas (with a flow rate of 10 mL/min for 20 min) was initially purged into the packed column to ensure that no other gases were detected in the effluent. Then, the desired gas mixture with a flow rate of 4 mL/min (MFC-5) was dosed into the column. Effluent from the bed was monitored by a gas chromatography (GC). The breakthrough time (dead volume time) for the sample bed filled with 0.5 mm glass beads and glass wool at 298 K is 11.4 minutes. The breakthrough time used in the draft is the raw time, without subtracting the time occupied by the dead volume. The gas separation capacities were determined by their amounts fed through the bed during the breakthrough time, respectively.

Mass Flow Controller (MFC-5) is calibrated for N_2. The conversion factor (CF) is as follows: CH_4 (0.763); C_2H_2 (0.615); C_2H_4 (0.619); C_2H_6 (0.49); C_3H_6 (0.505) and C_3H_8 (0.343).

For C_2H_2/C_2H_4 (1/99, v/v) mixture:

CF1 = 100/[(1/0.615)+(99/0. 619)]= 0.618965

The actual mixed gas flow rate = CF1*4 mL/min= 2.476 mL/min.

For C_2H_6/C_2H_4 (10/90, v/v) mixture:

CF1 = 100/[(10/0.49)+(90/0.619)]= 0.6031

The actual mixed gas flow rate = CF1*4 mL/min= 2.412 mL/min.

For $C_2H_2/C_2H_6/C_2H_4$ (1/9/90, v/v/v) mixture:

CF1 = 100/[(1/0.615)+(9/0.49)+(90/0.619)]= 0.6046

The actual mixed gas flow rate = CF1*4 mL/min= 2.419 mL/min.

Estimation of the isosteric heats of gas adsorption.

A virial-type expression comprising the temperature-independent parameters a_i and b_j was employed to calculate the enthalpies of adsorption for C_2H_2, C_2H_4 and C_2H_6 (288, 298 and 308 K) of **NTUniv-69A**. In each case, the data were fitted using the equation S1:

$$\ln P = \ln N + 1/T \sum_{i=0}^{m} a_i N^i + \sum_{j=0}^{n} b_j N^j \qquad \text{equation S1}$$

Here, P is the pressure expressed in Torr, N is the amount adsorbed in mmol/g, T is the temperature in K, a_i and b_j are virial coefficients, and m, n represent the number of coefficients required to adequately describe the isotherms (m and n were gradually increased until the contribution of extra added a and b coefficients was deemed to be statistically insignificant towards the overall fit, and the average value of the squared deviations from the experimental values was minimized). The values of the virial coefficients a_0 through a_m were then used to calculate the isosteric heat of adsorption using the following equation S2.

$$Q_{st} = -R \sum_{i=0}^{m} a_i N^i \qquad \text{equation S2}$$

Q_{st} is the coverage-dependent isosteric heat of adsorption and R is the universal gas constant.

Table S1. Parameters for C_2H_2, C_2H_4 and C_2H_6 isosteric heat calculation of **NTUniv-69A**

	C_2H_2	**C_2H_4**	**C_2H_6**
R	0.998914866037478	0.999940525065743	0.999960817168273
a0	-6590.61297044041	-4220.89455997849	-5184.81952258749
a1	129.775842788995	2364.02026573171	875.162203520054
a2	-15.3239850685299	0.198496435566625	-210.331743681698
a3	0.617991587742539	-0.00362553483973683	332.675504818875
a4	-0.00807527115125056	0	-80.162877903811
b0	25.3457020502505	16.8383361105917	20.2848877044039
b1	0	-7.68467289534668	-2.36734724358251

Table S2. Crystallographic data and structure refinement results for **NTUniv-69A**.

	NTUniv-69A
Formula	C6H3NO4Zn
Formula weight	217.46
Temperature/K	296
Crystal system	Orthorhombic
Space group	Ama2
a (Å)	21.073(3) Å
b (Å)	18.348(3) Å
c (Å)	5.8282(9) Å
α (°)	90°.
β (°)	90°.
γ (°)	90°.
V (Å^3)	2253.4(6) Å^3
Z	8
D_{calcd} (g cm^{-3})	1.282
F(000)	856
GOF	1.070
Final R indices [I>2sigma(I)]	R1 = 0.0786, wR2 = 0.2275
R indices (all data)	R1 = 0.0849, wR2 = 0.2397
Largest diff. peak and hole (e Å^{-3})	1.838 and -1.493 e.Å^{-3}

Table S3: Gas adsorption performances of some classical MOFs

	C_2H_6		C_2H_4		C_2H_2		Selectivities		Ref
	uptake	Q_{st}	uptake	Q_{st}	uptake	Q_{st}	C_2H_6/ C_2H_4	C_2H_2/ C_2H_4	
TJT-100	105	29	98	25	127	31	1.8	1.2	[1]
NOTT-300	19	25	95.8	45	142	47	13.6	1.87	[2]
Dy-MOF	\	\	93	21	109	26	\	1.1	[3]
dia-[Sc(Hpzc)	\	\	4	19.	7.3	37	\	3.1	[4]
FeMOF-74	\	\	134	45	127	47	\	2.08	[5]
ZJNU-14	\	\	89	31	72	35	\	1.59	[6]
NUC-19	\	\	32	29	76	30	\	4	[7]
ZJNU-119	\	\	101	24	134	26	\	3.5	[8]
Cu(TIA)	94	28	84	27	106	29	1.56	2.09	[8]
Zn-atz-ipa	45	46	35	40	\	\	1.67	\	[9]
Azole-Th-1	111	28	80	26	\	\	1.46	\	[10]
JNU-2	92	29	80	26	\	\	1.5	\	[11]
UiO-67(NH_2)$_2$	119	27	97	26	132	24	1.7	2.1	[12]
UPC-612	67	24	62	17	80	22	1.5	1.1	[13]
UPC-613	63	30	51	28	57	32	1.6	1.6	[13]
Zn(ad)(int)	52	33	\	29	\	34	2.4	2.4	[14]
[Zn(BDC)(H_2 BPZ)]	81	31	73	23	100	28	1.6	2.2	[15]

CuTiF6-TPPY	80	36	63	34	53	30	2	5	[16]
Zn-atz-oba	46	30		27		29	1.27	1.43	[17]

The unit for gas uptake was $cm^3\ g^{-1}$, the testing conditions was 298 K and 1 bar. The unit for Q_{st} was kJ mol^{-1}. The volume ratio for C_2H_6/C_2H_4 and C_2H_2/C_2H_4 was 1:9 and 1:99.

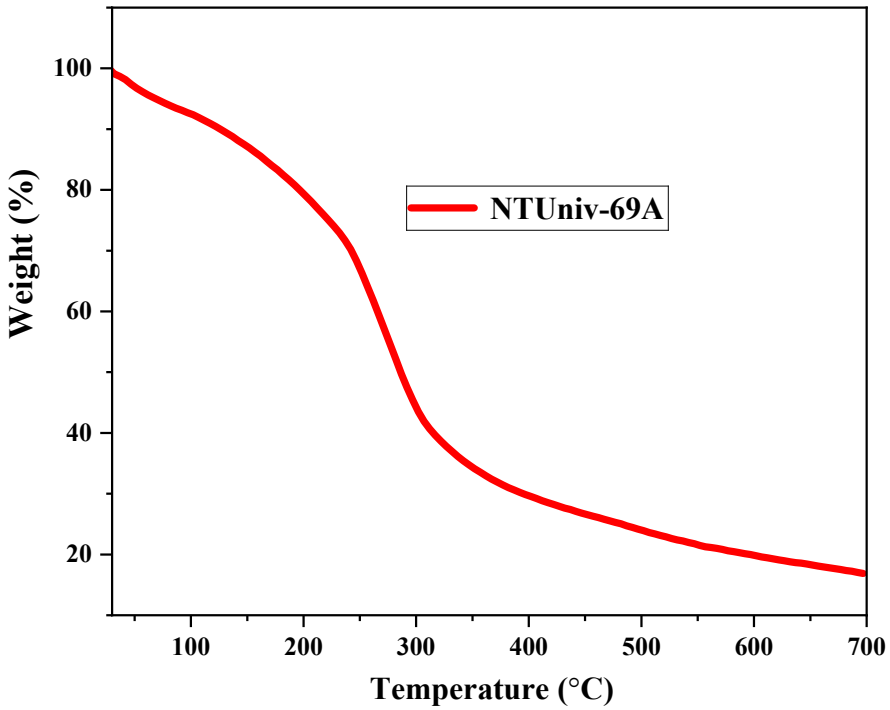

Figure S2. TGA data of as-synthesized **NTUniv-69A.**

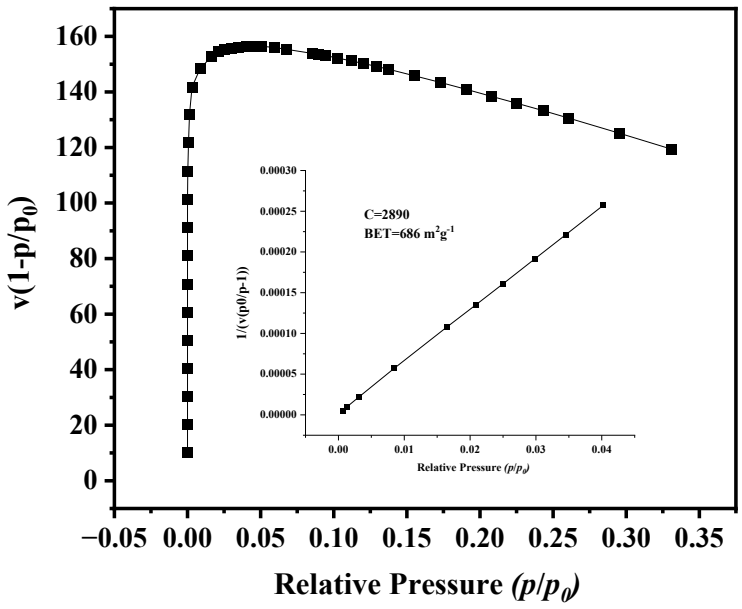

Figure S3. The BET plots for **NTUniv-69A** in the chosen range (P/P_0 = 0.001–0.03).

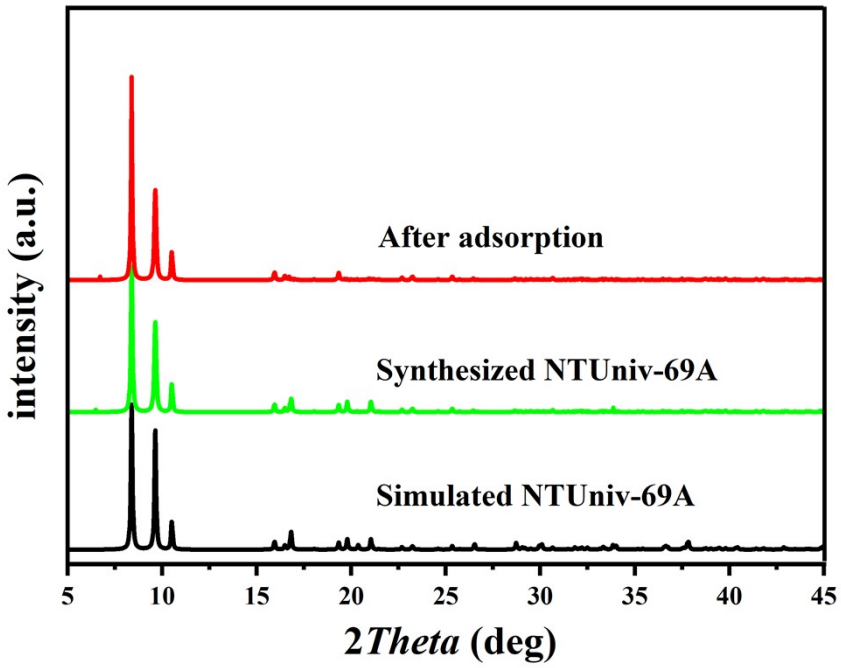

Figure S4. The PXRD patterns of **NTUniv-69A**. A simulated PXRD pattern from the single-crystal structure; synthesized and activated sample after adsorption, respectively.

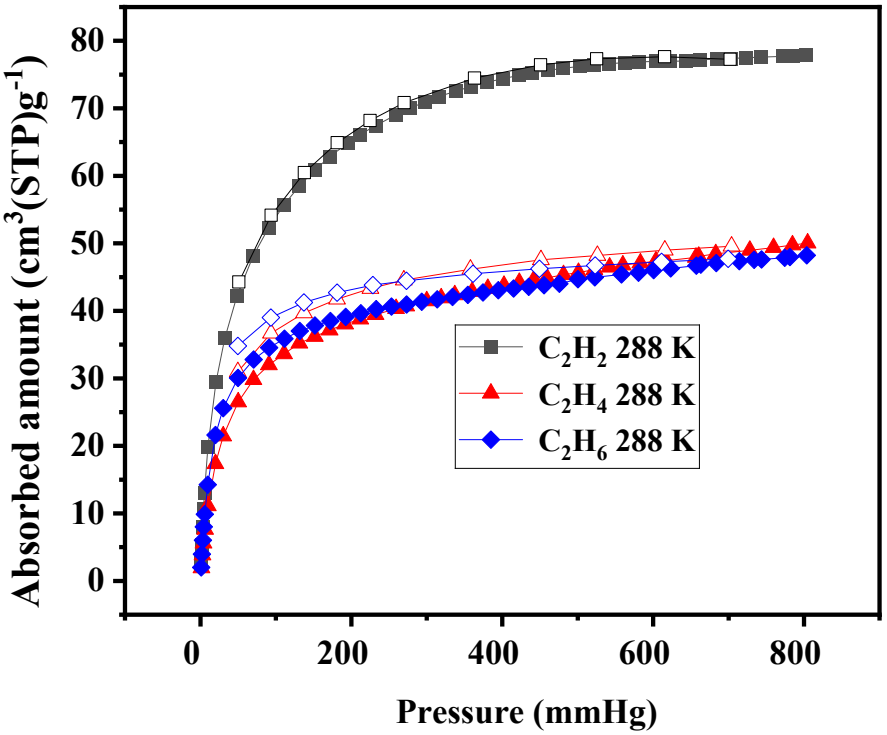

Figure S5. C_2H_2, C_2H_4 and C_2H_6 adsorption isotherms of **NTUniv-69A** collected at 288 K.

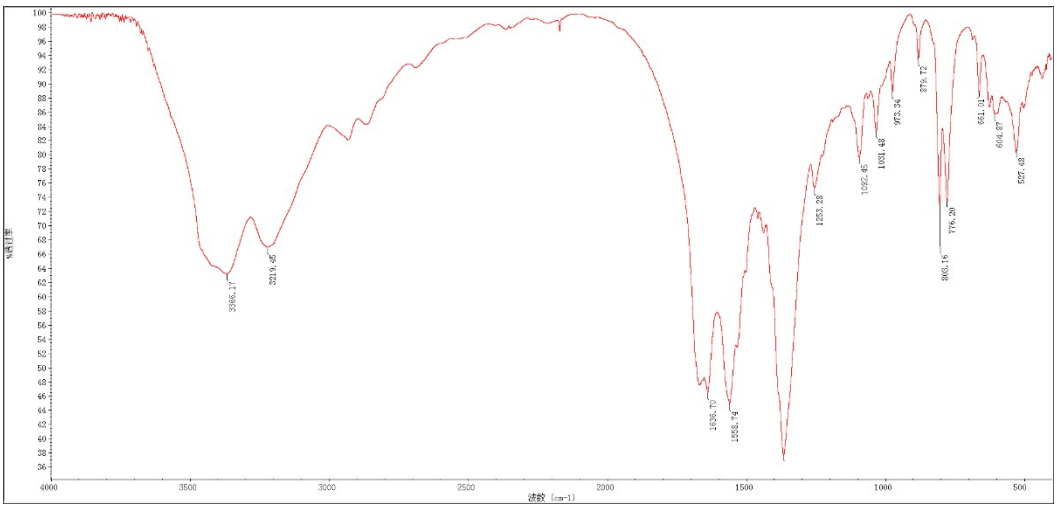

Figure S6. IR of the synthesized **NTUniv-69A**.

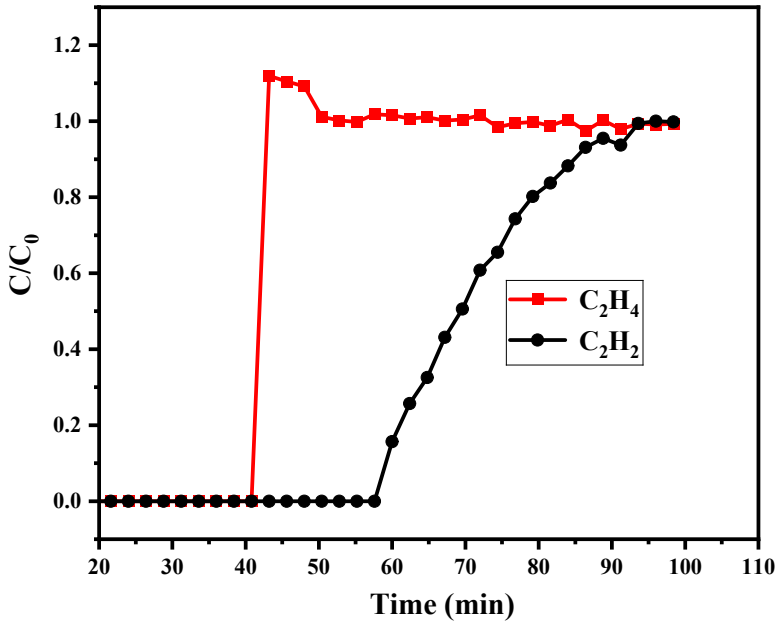

Figure S7. Experimental breakthrough curve at 298 K and 1 bar for C_2H_2/C_2H_4 (1/99, v/v) for **NTUniv-69A** (1.243 g).

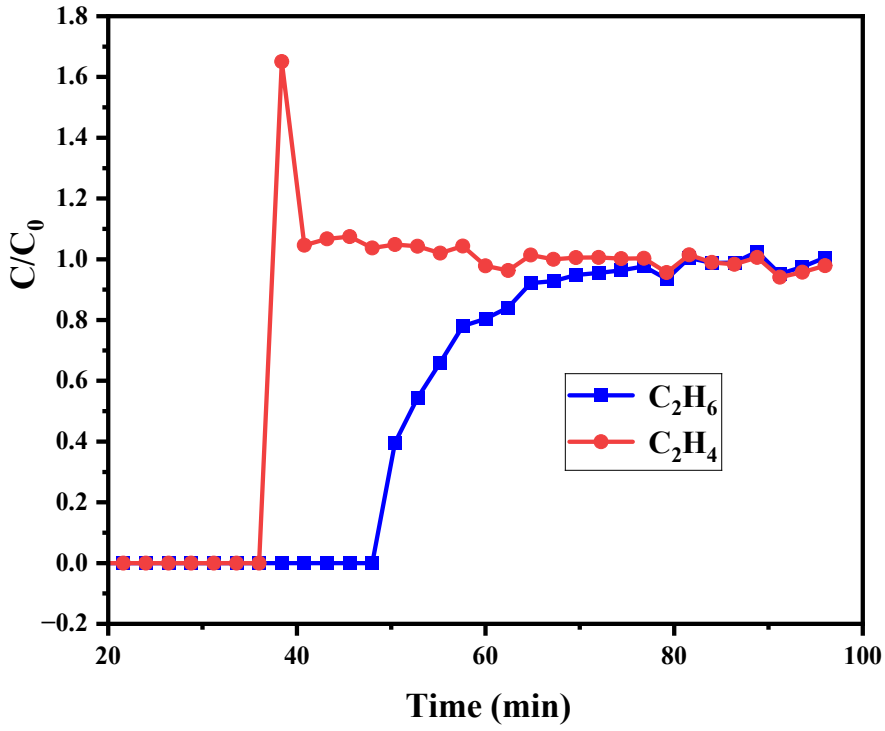

Figure S8. Experimental breakthrough curve at 298 K and 1 bar for C_2H_6/C_2H_4 (10/90, v/v) for **NTUniv-69A** (1.243 g).

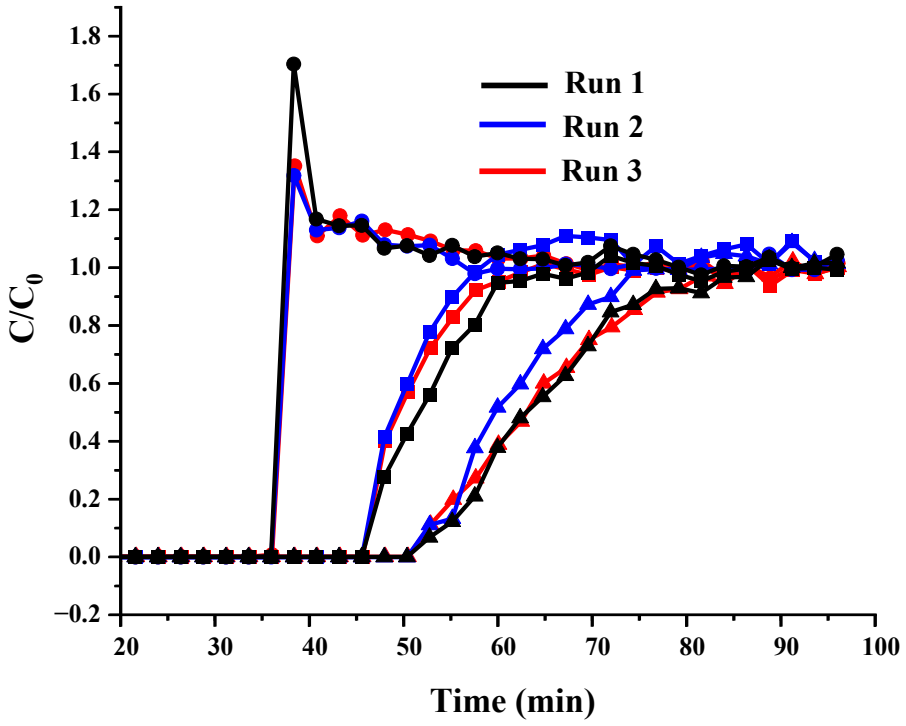

Figure S9. Experimental breakthrough curve at 298 K and 1 bar for $C_2H_2/C_2H_6/C_2H_4$ (1/9/90, v/v/v) for **NTUniv-69A** (1.243 g).

Prediction of the gas adsorption selectivity by IAST

IAST (ideal adsorption solution theory) was used to predict binary mixture adsorption from the experimental pure-gas isotherms. To perform the integrations required by IAST, the single-component isotherms should be fitted by a proper model. In practice, several methods to do this are available. We found for this set of data that the dual-site Langmuir-Freundlich (DSLF) equation was successful in fitting the data. As can be seen in the following tables, the model fits the isotherms very well (R^2 > 0.99999).

$$q = \frac{q_{m,1} b_1 p^{1/n_1}}{1 + b_1 p^{1/n_1}} + \frac{q_{m,2} b_2 p^{1/n_2}}{1 + b_2 p^{1/n_2}} \qquad \text{equation S3}$$

Here, P is the pressure of the bulk gas at equilibrium with the adsorbed phase (kPa),

q (equation S3) is the adsorbed amount per mass of adsorbent (mmol/g), $q_{m,1}$ and $q_{m,2}$ are the saturation capacities of sites 1 and 2 (mmol/g), b_1 and b_2 are the affinity coefficients of sites 1 and 2 (1/kPa), and n_1 and n_2 represent the deviations from an ideal homogeneous surface. The fitted parameters were then used to predict multi-component adsorption with IAST.

The selectivity $S_{A/B}$ in a binary mixture of components A and B is defined as $(x_A/y_A)/ (x_B/y_B)$, where xi and yi are the mole fractions of component i (i = A, B) in the adsorbed and bulk phases, respectively.

Table S4. Dual-site Langmuir-Freundlich parameters for pure C_2H_2, C_2H_4 and C_2H_6 isotherms in **NTUniv-69A** at 298 K

	C_2H_2	C_2H_4	C_2H_6
R^2	0.999760855335752	0.999955330015456	0.99992005403069
$q_{m,1}$	2.83127161591899	1.47208555856674	400935.158116894
$q_{m,2}$	0.64141356353163	1.6212355267269	1.93335293460717
b_1	0.166263113526925	0.184180582311789	2.96933902690474E-9
b_2	6.24563323381866E-5	0.016352050911085	0.222651036843428
n_1	0.970566792924761	1.14458818478387	1.13572487858384
n_2	2.78012890379895	0.804668844193367	1.13500621370028

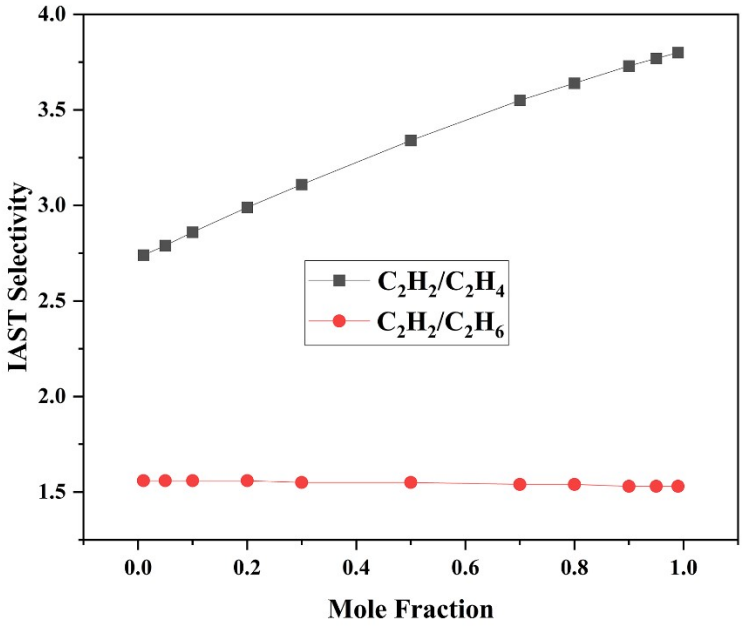

Figure S10. IAST selectivities of C_2H_2/C_2H_4 and C_2H_6/C_2H_4 as a function of gas mole fraction at 298 K and 1 bar, calculated based on the DSLF fitting parameters listed in Table S4.

Modeling Studies

Atomistic GCMC simulations were performed for C_2H_2, C_2H_4 and C_2H_6 in **NTUniv-69A**. The optimized structures are in great consistency with the experimentally determined crystal structures. All simulations/calculations were performed by the Materials Studio 7.0 package according to the literature[18]. The adsorption location of C_2H_2, C_2H_4 and C_2H_6 were estimated through Grand Canonical Monte Carlo (GCMC) simulations by using the location task, adsorption isotherm task and metropolis method[19] in the sorption calculation module. The framework and gas molecules were regarded as rigid[20]. All atom charges of the framework were assigned by the COMPASSII field[18b, 21]. The ESP charges calculated by DFT were employed to guest atoms[22]. The cutoff distance was set to 12.5 Å for the Lennard-Jones (LJ) interactions, and the electrostatic interactions and the van der Waals interactions were handled using the Ewald and Atom based summation method, respectively. The loading steps, production steps and temperature cycles were set to 1×10^6, 1×10^7 and 40, respectively.

The preferred adsorption sites of guest molecules were searched through GCMC simulations to produce a preliminary host–guest configuration. Then the unit-cell of this host-guest structure was optimized by TD-DFT/Dmol^3. The binding energies between the frameworks and C_2H_2, C_2H_4 and C_2H_6 gas molecules at special adsorption sites were calculated through DFT simulations by using the energy task in the Dmol^3 module, using the generalized gradient approximation (GGA) with the Perdew-Burke-Ernzerhof (PBE) functional[23] and the double numerical plus d-functions (DNP) basis set, TS for DFT-D correction, and the All Electron. The related models were extracted from MOF with guest molecules being located at primary sites after the "location" task. The binding energy is expressed as $E_{binding} = E(\text{MOF})+E(\text{gas})-E(\text{MOF+gas})$.

1.Hao, H.-G.; Zhao, Y.-F.; Chen, D.-M.; Yu, J.-M.; Tan, K.; Ma, S.; Chabal, Y.; Zhang, Z.-M.; Dou, J.-M.; Xiao, Z.-H.; Day, G.; Zhou, H.-C.; Lu, T.-B., Simultaneous Trapping of C2H2 and C2H6 from a Ternary Mixture of C2H2/C2H4/C2H6 in a Robust Metal–Organic Framework for the Purification of C2H4. *Angew. Chem. Int. Ed.* **2018,** *57* (49), 16067-16071.

2.Yang, S.; Ramirez-Cuesta, A. J.; Newby, R.; Garcia-Sakai, V.; Manuel, P.; Callear, S. K.; Campbell, S. I.; Tang, C. C.; Schroder, M., Supramolecular binding and separation of hydrocarbons within a functionalized porous metal-organic framework. *Nat Chem* **2014,** *7* (2), 121-9.

3.Li, Y.-Z.; Wang, H.-H.; Wang, G.-D.; Hou, L.; Wang, Y.-Y.; Zhu, Z., A Dy6-cluster-based fcu-MOF with efficient separation of C2H2/C2H4 and selective adsorption of benzene. *Inorg. Chem. Front.* **2021,** *8* (2), 376-382.

4.Barsukova, M. O.; Kovalenko, K. A.; Nizovtsev, A. S.; Sapianik, A. A.; Samsonenko, D. G.; Dybtsev, D. N.; Fedin, V. P., Isomeric Scandium–Organic Frameworks with High Hydrolytic Stability and Selective Adsorption of Acetylene. *Inorg. Chem.* **2021,** *60* (5), 2996-3005.

5.Bloch, E. D.; Queen, W. L.; Krishna, R.; Zadrozny, J. M.; Brown, C. M.; Long, J. R., Hydrocarbon separations in a metal-organic framework with open iron(II) coordination sites. *Science* **2012,** *335* (6076), 1606-10.

6.Jiang, Z.; Fan, L.; Zhou, P.; Xu, T.; Chen, J.; Hu, S.; Chen, D.-L.; He, Y., An N-oxide-functionalized nanocage-based copper-tricarboxylate framework for the selective capture of C2H2. *Dalton Trans* **2020,** *49* (44), 15672-15681.

7.Chen, H.; Feng, L.; Zhang, X.; Gao, Z.-Y.; Sun, D., Robust Heterometallic CoIILaIII2–Organic Framework for the Highly Efficient Separation of Acetylene from Light Hydrocarbon Mixtures. *Inorg. Chem.* **2021,** *60* (5), 2878-2882.

8.Zhou, P.; Wang, X.; Yue, L.; Fan, L.; He, Y., A Microporous MOF Constructed by Cross-Linking Helical Chains for Efficient Purification of Natural Gas and Ethylene. *Inorg. Chem.* **2021,** *60* (19), 14969-14977.

9.Zhang, M.; Zhao, H.; Wang, Y.; Jiang, J.; Chen, M.; He, X.; Liu, P.; Dang, R.; Cui, H.; Wang, M.; Sun, T.; Qin, G.; Tang, Y.; Wang, S., Fine-Tuning MOFs with Amino Group for One-Step Ethylene Purification from the C2 Hydrocarbon Mixture. *Inorg. Chem.* **2023,** *62* (21), 8428-8434.

10.Xu, Z.; Xiong, X.; Xiong, J.; Krishna, R.; Li, L.; Fan, Y.; Luo, F.; Chen, B., A robust Th-azole framework for highly efficient purification of C2H4 from a C2H4/C2H2/C2H6 mixture. *Nat Commun* **2020,** *11* (1), 3163.

11.Zeng, H.; Xie, X.-J.; Xie, M.; Huang, Y.-L.; Luo, D.; Wang, T.; Zhao, Y.; Lu, W.; Li, D., Cage-Interconnected Metal–Organic Framework with Tailored Apertures for Efficient C2H6/C2H4 Separation under Humid Conditions. *J. Am. Chem. Soc.* **2019,** *141* (51), 20390-20396.

12.Gu, X.-W.; Wang, J.-X.; Wu, E.; Wu, H.; Zhou, W.; Qian, G.; Chen, B.; Li, B., Immobilization of Lewis Basic Sites into a Stable Ethane-Selective MOF Enabling One-Step Separation of Ethylene from a Ternary Mixture. *J. Am. Chem. Soc.* **2022,** *144* (6), 2614-2623.

13.Wang, Y.; Hao, C.; Fan, W.; Fu, M.; Wang, X.; Wang, Z.; Zhu, L.; Li, Y.; Lu, X.; Dai, F.; Kang, Z.; Wang, R.; Guo, W.; Hu, S.; Sun, D., One-step Ethylene Purification from an Acetylene/Ethylene/Ethane Ternary Mixture by Cyclopentadiene Cobalt-Functionalized Metal–

Organic Frameworks. *Angew. Chem. Int. Ed.* **2021,** *60* (20), 11350-11358.
14.Ding, Q.; Zhang, Z.; Liu, Y.; Chai, K.; Krishna, R.; Zhang, S., One-Step Ethylene Purification from Ternary Mixtures in a Metal–Organic Framework with Customized Pore Chemistry and Shape. *Angew. Chem. Int. Ed.* **2022,** *61* (35), e202208134.
15.Wang, G.-D.; Li, Y.-Z.; Shi, W.-J.; Hou, L.; Wang, Y.-Y.; Zhu, Z., One-Step C2H4 Purification from Ternary C2H6/C2H4/C2H2 Mixtures by a Robust Metal–Organic Framework with Customized Pore Environment. *Angew. Chem. Int. Ed.* **2022,** *61* (28), e202205427.
16.Zhang, P.; Zhong, Y.; Zhang, Y.; Zhu, Z.; Liu, Y.; Su, Y.; Chen, J.; Chen, S.; Zeng, Z.; Xing, H.; Deng, S.; Wang, J., Synergistic binding sites in a hybrid ultramicroporous material for one-step ethylene purification from ternary C₂ hydrocarbon mixtures. *Sci. Adv* **2022,** *8* (23), eabn9231.
17.Cao, J.-W.; Mukherjee, S.; Pham, T.; Wang, Y.; Wang, T.; Zhang, T.; Jiang, X.; Tang, H.-J.; Forrest, K. A.; Space, B.; Zaworotko, M. J.; Chen, K.-J., One-step ethylene production from a four-component gas mixture by a single physisorbent. *Nat Commun* **2021,** *12* (1), 6507.
18.a）Li, Y.-W.; Yan, H.; Hu, T.-L.; Ma, H.-Y.; Li, D.-C.; Wang, S.-N.; Yao, Q.-X.; Dou, J.-M.; Xu, J.; Bu, X.-H., Two microporous Fe-based MOFs with multiple active sites for selective gas adsorption. *Chem. Commun.* **2017,** *53* (15), 2394-2397; b）Song, X.; Zhang, M.; Chen, C.; Duan, J.; Zhang, W.; Pan, Y.; Bai, J., Pure-Supramolecular-Linker Approach to Highly Connected Metal–Organic Frameworks for CO2 Capture. *J. Am. Chem. Soc.* **2019,** *141* (37), 14539-14543.
19.Metropolis, N.; Ulam, S., The Monte Carlo Method. *J Am Stat Assoc* **1949,** *44* (247), 335-341.
20.a）Wu, Y.; Chen, H.; Liu, D.; Qian, Y.; Xi, H., Adsorption and separation of ethane/ethylene on ZIFs with various topologies: Combining GCMC simulation with the ideal adsorbed solution theory (IAST). *Chem. Eng. Sci.* **2015,** *124*, 144-153; b）Zhang, P.; Zhong, Y.; Zhang, Y.; Zhu, Z.; Liu, Y.; Su, Y.; Chen, J.; Chen, S.; Zeng, Z.; Xing, H.; Deng, S.; Wang, J., Synergistic binding sites in a hybrid ultramicroporous material for one-step ethylene purification from ternary C2 hydrocarbon mixtures. *Sci. Adv* **2022,** *8* (23), eabn9231.
21.a）Sun, H.; Jin, Z.; Yang, C.; Akkermans, R. L. C.; Robertson, S. H.; Spenley, N. A.; Miller, S.; Todd, S. M., COMPASS II: extended coverage for polymer and drug-like molecule databases. *J. Mol. Model.* **2016,** *22* (2), 47; b）Cheng, H.; Wang, Q.; Meng, L.; Sheng, P.; Zhang, Z.; Ding, M.; Gao, Y.; Bai, J., Formation of a N/O/F-Rich and Rooflike Cluster-Based Highly Stable Cu(I/II)-MOF for Promising Pipeline Natural Gas Upgrading by the Recovery of Individual C3H8 and C2H6 Gases. *ACS Appl. Mater. Interfaces* **2021,** *13* (34), 40713-40723.
22.a）Liao, P.-Q.; Huang, N.-Y.; Zhang, W.-X.; Zhang, J.-P.; Chen, X.-M., Controlling guest conformation for efficient purification of butadiene. *Science* **2017,** *356* (6343), 1193-1196; b）Wang, Z.-Q.; Luo, H.-Q.; Wang, Y.-L.; Xu, M.-Y.; He, C.-T.; Liu, Q.-Y., Octanuclear Cobalt(II) Cluster-Based Metal–Organic Framework with Caged Structure Exhibiting the Selective Adsorption of Ethane over Ethylene. *Inorg. Chem.* **2021,** *60* (14), 10596-10602.
23.Perdew, J. P.; Burke, K.; Ernzerhof, M., Generalized Gradient Approximation Made Simple. *Phys. Rev. Lett.* **1996,** *77* (18), 3865-3868.